Spatial Variation of Crustal Attenuation Properties in Western Tibet

Rahul Biswas & Chandrani Singh

Department of Geology and Geophysics, Indian Institute of Technology Kharagpur

INTRODUCTION

1. In this study coda (Q_C^{-1}), intrinsic (Q_i^{-1}) and scattering (Q_{SC}^{-1}) attenuation are calculated using local earthquakes recorded during 2007 to 2011.
2. Single isotropic model by Sato (1977) is used to calculate the coda wave attenuation (Q_C^{-1}).
3. Multiple Lapse Time Window Analysis (MLTWA) is used to separate the values of intrinsic (Q_i^{-1}) and scattering (Q_{SC}^{-1}) attenuation.

STUDY AREA

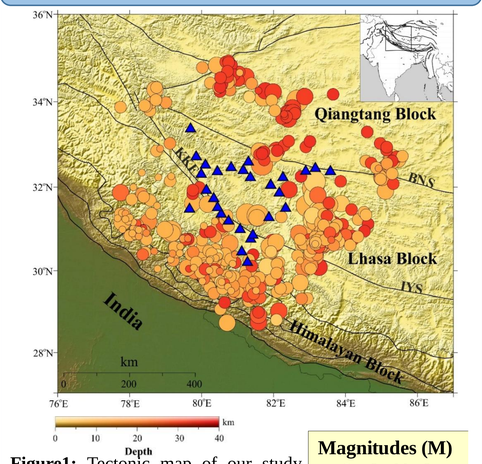

Figure1: Tectonic map of our study area that includes locations of the Earthquakes (circles) and stations (triangles) used in the present study.

Magnitudes (M)
- 2 < M < 3
- 3 < M < 4
- 4 < M < 5
- 5 < M < 6
- 6 < M

OBJECTIVES

1. Estimation of the values of coda, intrinsic and scattering attenuation using single isotropic model and MLTWA respectively at different frequencies for each station.
2. To obtain a spatial map of attenuation parameters for better understanding of attenuation mechanism.
3. Compare the obtained results with the other tectonically active regions worldwide.

NUMERICAL MODEL

$$E_{gm}(r,t) \approx \frac{W_0\, exp[-vLe^{-1}t]}{4\pi r^2 v}\,\delta\left[t-\frac{r}{v}\right] + W_0 H\left[t-\frac{r}{v}\right].\frac{\left(1-\frac{r^2}{v^2t^2}\right)^{\frac{1}{8}}}{\left(\frac{4\pi vt}{3B_0Le^{-1}}\right)^{\frac{3}{2}}}$$

$$\times$$

$$exp[-vLe^{-1}t].G\left[vLe^{-1}tB_0\left(1-\frac{r^2}{v^2t^2}\right)^{3/4}\right]$$

$$B_0 = \frac{Q_{SC}^{-1}}{Q_{SC}^{-1}+Q_i^{-1}} \quad Le = \frac{1}{Q_{SC}^{-1}+Q_i^{-1}} \quad G(x) = e^x\sqrt{1+2.026/x}$$

Here, E_{gm} is the energy of ground motion. W_0 is the energy at source; v is the velocity in the half-space; H is the Heaviside function; δ is Dirac's delta, r is the source receiver distance

DATA & METHODOLOGY

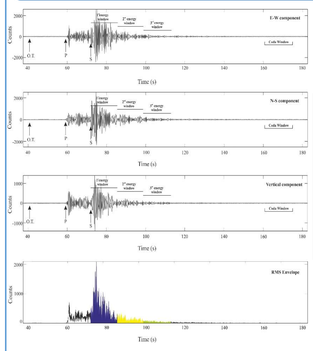

Figure2:. Example of one event (3 components) recorded by GUGE station.

Low Freq.	Central Freq.	High Freq.
1	1.5	2
2	3	4
4	6	8
8	12	16
12	18	24

Table1: Frequency characteristics table used in this study

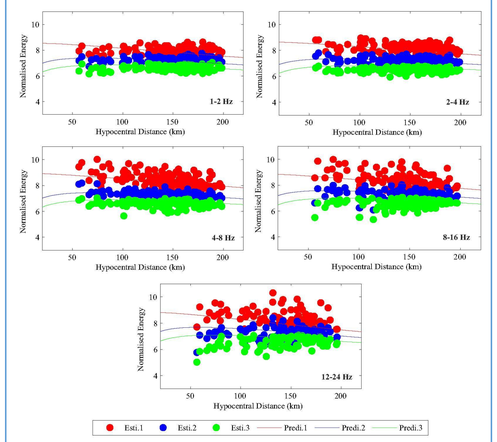

Figure3: Plots repre- sents Normalized energy for GUGE station area at five frequencies. Different colours stand for the different energy measurements such as red for the 0–15 s, blue for 15–30 s and green for 30–45 s respectively. The predictions for the best fit to obtain B_0 and Le^{-1} are represented by solid lines. Est.-Estimated; Predi.-Predicted.

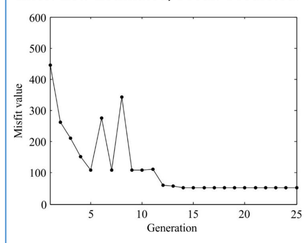

Figure4: Misfit values at 3 Hz. It decreases with iteration.

$$E_k^{obs}[r_i] = \int_{t_{Si}+(k-1)\Delta t}^{t_{Si}+k\Delta t} E_S[r_i,t]dt \qquad EN_k^{obs}[r_i] = 4\pi {r_i}^2 \frac{E_k^{obs}[r_i]}{E_{coda}^{obs}[r_i]}, k = 1,2,3$$

$$E_{coda}^{obs}[r_i] = \int_{t_{coda}}^{t_{coda}+\Delta t} E_S[r_i,t]dt \qquad E_k^{th}[r_i] = 4\pi {r_i}^2 \frac{\int_{(r_i/v)+(k-1)\Delta t}^{(r_i/v)+k\Delta t} E_{gm}[r_i,t]dt}{\int_{t_c}^{t_c+\Delta t} E_{gm}[r_i,t]dt}$$

$$k=1,2,3$$

$$LsM[B_0, Le^{-1}] = \sum_{k=1}^{3}\sum_{i=1}^{N} |log[EN_k^{obs}(r_i)] - log[EN_k^{obs}(r_i)]|^2$$

RESULTS

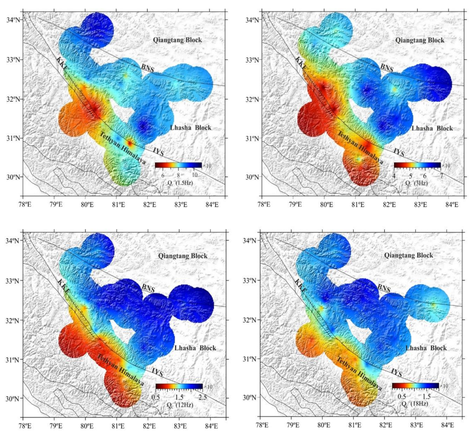

Figure5: Spatial distribution of coda Q^{-1} for different frequency band.

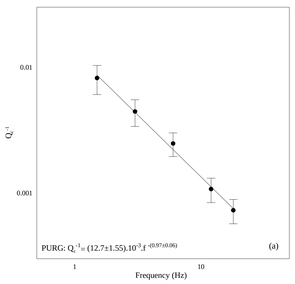

Figure6a: Plot of estimated values Q_C^{-1} as a function of frequency.

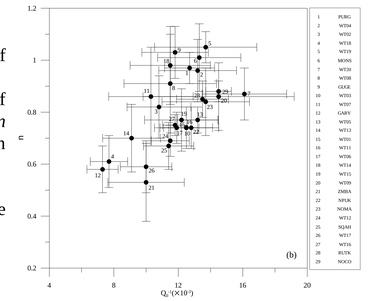

Figure6b:. (b) Plot of estimated values of Q_C^{-1} and n for each station together with the associated errors.

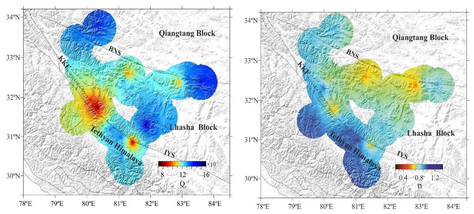

Figure7: Spatial distribution of coda Q^{-1} at 1 Hz frequency and n for this study area.

RESULTS

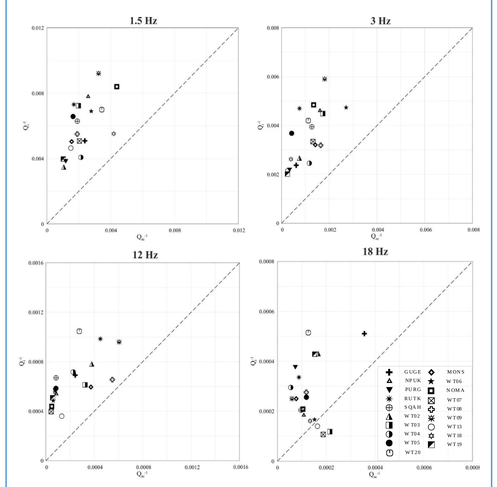

Figure8: Plot of Q_i^{-1} versus Q_{SC}^{-1} at different frequencies for all analysed stations. The dashed line represents $Q_i^{-1} = Q_{SC}^{-1}$.

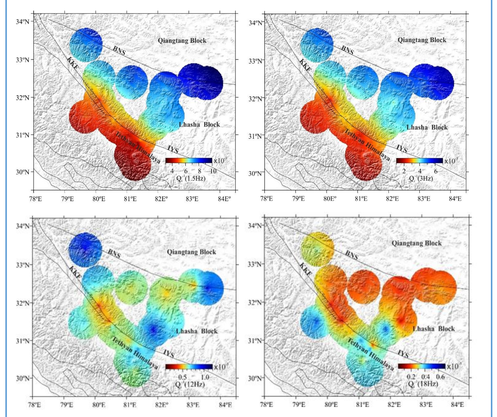

Figure9: Spatial distribution of Q_i^{-1} at different central frequency band.

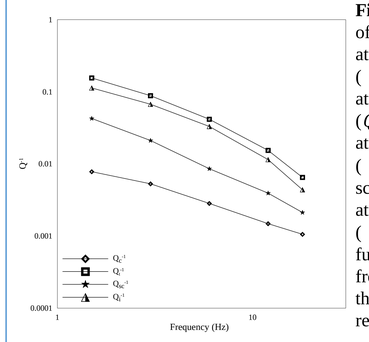

Figure10: Plot of coda wave attenuation (Q_C^{-1}), total attenuation (Q_t^{-1}), intrinsic attenuation (Q_i^{-1}) and scattering attenuation (Q_{SC}^{-1}) as a function of frequency for the study region.

WORLDWIDE COMPARISON

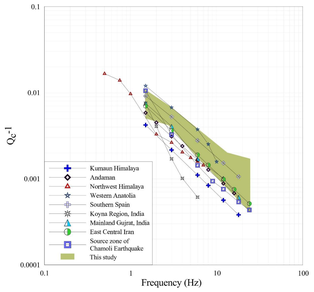

Figure11a: Comparing the obtained values of Q_C^{-1} with the values obtained worldwide and India.

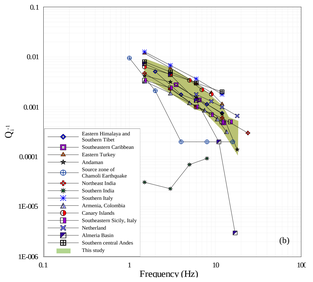

Figure11b: Comparing the obtained values of Q_i^{-1} with the values obtained worldwide and India.

CONCLUSIONS

- Q_C values are found to be frequency dependent at all stations and intrinsic attenuation prevails over scattering attenuation except few station at 18 Hz.
- Intrinsic attenuation is observed to be high in upper portion of western Tibet compared to the lower portion.
- The obtained values of Q are well comparable with the other results obtained for the same tectonic regime.

REFERENCES

1. Del Pezzo, Edoardo, and Francesca Bianco. "MathLTWA: Multiple lapse time window analysis using Wolfram Mathematica 7." *Computers & Geosciences* 36, no. 10 (2010): 1388-1392.
2. Sato, Haruo. "Energy propagation including scattering effects single isotropic scattering approximation." *Journal of Physics of the Earth* 25.1 (1977): 27-41.
3. Singh, S., Singh, C., Biswas, R., Mukhopadhyay, S. and Sahu, H., 2016. Attenuation characteristics in eastern Himalaya and southern Tibetan Plateau: An understanding of the physical state of the medium. *Physics of the Earth and Planetary Interiors*, *257*, pp.48-56.
4. Singh, C., Biswas, R., Srijayanthi, G. and Kumar, M.R., 2017. Relative role of intrinsic and scattering attenuation beneath the Andaman Islands, India and tectonic implications. *Physics of the Earth and Planetary Interiors*, *271*, pp.19-28.

ACKNOWLEDGEMENTS:

We acknowledge IRIS DMC for providing the data. We also thank the Department of Geology and Geophysics, IIT Kharagpur for their assistance in this research.